

Supporting Information

Halogenated Building Blocks for 2D Crystal Engineering on Solid Surfaces: Lessons from Hydrogen Bonding

*Arijit Mukherjee,^{†#} Ana Sanz-Matias,^{##} Gangamallaiiah Velpula,[†] Deepali Waghray,[†] Oleksandr Ivasenko,[†] Nerea Bilbao,[†] Jeremy Harvey,^{**} Kunal S. Mali,^{*†} and Steven De Feyter^{†*}*

[†]Division of Molecular Imaging and Photonics, Department of Chemistry, KU Leuven, Celestijnenlaan, 200F, B-3001 Leuven, Belgium, ^{*}Quantum Chemistry and Physical Chemistry, Department of Chemistry, KU Leuven, BE-3001 Leuven, Belgium

[#]These authors contributed equally

Corresponding authors: jeremy.harvey@kuleuven.be, kunal.mali@kuleuven.be,
steven.defeyter@kuleuven.be

Contents:

1. Synthesis and characterization of molecules used in the study.
2. Natural bonding orbitals (NBO) analysis of halogen bonding (Figure S1, Table S1).
3. One-dimensional periodic DFT calculations (Figure S2, Table S2).
4. Additional STM data (Figure S3, S4, S5).
5. Effect of the inclusion of the extra-site (Table S3, S4, S5).
6. Alkyl chain distance and orientation on graphite (Table S6, Figure S6, Figure S7).
7. Periodic structure optimization and commensurability.
8. Estimation of alkyl chain contribution to stabilization (Figure S8).
9. Alkylated isophthalic acid models (Figure S9).
10. Double row (DR) *versus* zig-zag (ZZ) structures of **Br₂-C₆H₃-OC₁₂O-C₆H₃-Br₂** (Table S9, Figure S10).
11. Appendix: Program used to calculate the commensurability between two lattices.

Section 1. Synthesis of compounds:**General Experimental**

NMR spectra were acquired on commercial instrument (Bruker Avance II 600 MHz) and chemical shifts (δ) are reported in parts per million (ppm) referenced to tetramethylsilane (^1H). For column chromatography, 70-230 mesh silica 60 (E. M. Merck) was used as the stationary phase. Chemicals received from commercial sources (Acros Organic and Sigma-Aldrich) were used without further purification. All solvents were used as received from commercial sources and not explicitly dried prior to use ($\text{H}_2\text{O} \leq 0.1\%$).

Experimental and Characterization data

1,12-bis[3,5-di(carboxy)phenoxy]dodecane 5 was prepared following a previously reported procedure.¹

1,3-dibromo-5-(octyloxy)benzene 1: To a solution of 3,5-dibromophenol (0.50 g, 1.98 mmol) in 2-butanone (20 mL), potassium carbonate (1.3 g, 9.92 mmol) was added and the reaction mixture was stirred at room temperature for 30 min, then 1-bromooctane (0.64 mL, 3.96 mmol) was added and the reaction mixture was refluxed for 12 hours. After being cooled to room temperature the solid was filtered and solvent was concentrated under reduced pressure. The residue was then re-dissolved in diethyl ether, washed with water and brine, dried over anhydrous MgSO_4 and evaporated to dryness. Purification by column chromatography using petroleum ether gave compound **1** (0.620 g, 86 %) as a colourless liquid. ^1H NMR (600 MHz, CDCl_3): δ 7.21 (t, $J = 1.4$ Hz, 1H), 6.97 (d, $J = 1.4$ Hz, 2H), 3.90 (t, $J = 6.5$ Hz, 2H), 1.76-1.72 (m, 2H), 1.53-1.41 (m, 2H), 1.39-1.28 (m, 8H), 0.88 (t, $J = 6.5$ Hz, 3H). ^{13}C NMR (75 MHz, CDCl_3) δ (ppm) = 160.6, 126.3, 123.1, 117.1, 68.8, 32.9, 31.8, 29.3, 29.2, 29.1, 28.3, 26.0, 22.7, 14.0. MS (ESI+): 364.9 [M+H]⁺.

1,3-dibromo-5-(dodecyloxy)benzene 2: Synthesis according to procedure leading to compound **1**. 3,5-dibromophenol (0.50 g, 1.98 mmol), 2-butanone (20 mL), potassium carbonate (1.3 g, 9.92 mmol) and 1-bromododecane (0.95 mL, 3.96 mmol). Compound **2** (0.44 g, 53%) was obtained as a colorless liquid. ^1H NMR (600 MHz, CDCl_3): δ 7.22 (t, $J = 1.8$ Hz, 1H), 6.87 (d, $J = 1.8$ Hz, 2H), 3.90 (t, $J = 7.0$ Hz, 2H), 1.76-1.73 (m, 2H), 1.43-1.41 (m, 2H), 1.29-1.26 (m, 16 H), 0.88 (t, $J = 7.0$ Hz, 3H). ^{13}C NMR (100 MHz, CDCl_3) δ (ppm) = 160.4, 126.1, 123.1, 116.9, 68.6, 34.0, 32.9, 31.9, 29.6, 29.5, 29.4, 29.3, 29.0, 28.8, 28.2, 25.9, 22.7, 14.1. MS (ESI+): 421.1 [M+H]⁺.

1,3-dibromo-5-(octadecyloxy)benzene 3: Synthesis according to procedure leading to compound **1**. 3,5-dibromophenol (0.50 g, 1.98 mmol), 2-butanone (20 mL), potassium carbonate (1.3 g, 9.92 mmol) and 1-bromooctadecane (1.35 mL, 3.96 mmol). Compound **3** (0.870 g, 87%) was obtained as an off-white solid. ^1H NMR (600 MHz, CDCl_3): δ 7.22 (t, $J = 1.8$ Hz, 1H), 6.97 (d, $J = 1.8$ Hz, 2H), 3.90 (t,

$J = 6.9$ Hz, 2H), 1.76-1.73 (m, 2H), 1.43-1.41 (m, 2H), 1.33-1.25 (m, 28 H), 0.87 (t, $J = 6.9$ Hz, 3H).). ^{13}C NMR (75 MHz, CDCl_3) δ (ppm) = 160.5, 126.2, 123.0, 117.1, 68.7, 31.8, 29.7-29.5, 29.4, 29.3, 29.2, 29.0, 25.8, 22.6, 13.9. MS (ESI+): 505.2 $[\text{M}+\text{H}]^+$.

1,12-bis(3,5-dibromophenoxy)dodecane 4: Synthesis according to procedure leading to compound 1. 1,12-dibromododecane (0.250 g, 0.76 mmol), 3,5-dibromophenol (0.478 g, 1.90 mmol), 2-butanone (20 mL), potassium carbonate (1.05 g, 7.60 mmol). Compound 4 (0.425 g, 83 %) was obtained as an off-white solid. ^1H NMR (600 MHz, CDCl_3): δ 7.22 (t, $J = 1.4$ Hz, 2H), 6.97 (d, $J = 1.4$ Hz, 4H), 3.90 (t, $J = 6.6$ Hz, 4H), 1.76-1.73 (m, 4H), 1.42-1.41 (m, 4H), 1.33-1.28 (m, 12 H). ^{13}C NMR (100 MHz, CDCl_3): δ 160.4, 126.2, 123.1, 116.9, 68.6, 30.9, 29.5-29.4, 29.3, 29.0, 25.9. MS (ESI+): 671.2 $[\text{M}+\text{H}]^+$.

Section 2. NBO analysis of halogen bonding

2.1 Two-electron stabilization energies obtained from NBO and perturbation theory analysis on four representative dimers.

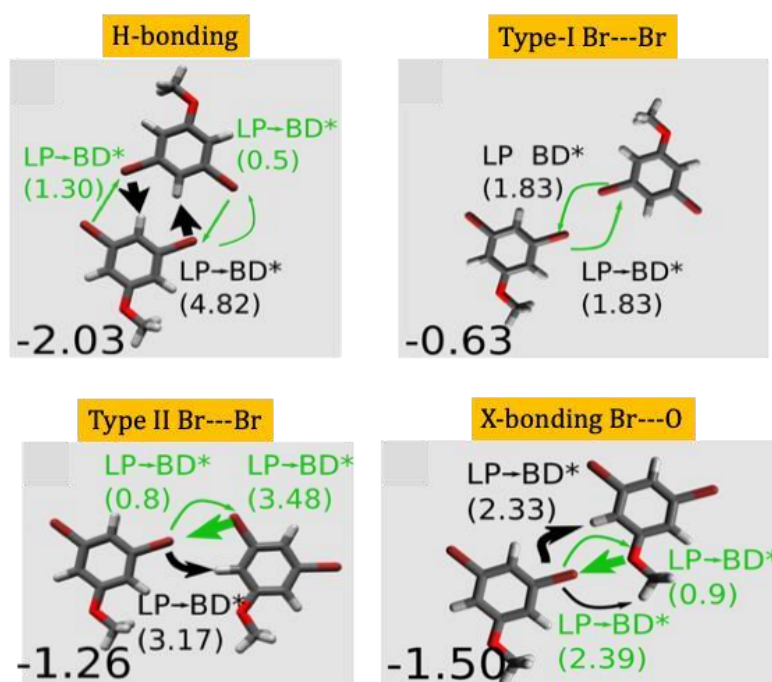


Figure S1. Schematic describing the main $\text{Br}_2\text{-C}_6\text{H}_3\text{-OMe}$ NBO stabilization energies $E(2)$. Black and green arrows and labels indicate respectively the main NBO stabilization energies $E(2)$ corresponding to unconventional hydrogen bonds and halogen bonds (in parenthesis, in kcal/mol) and the labels of the involved charge transfer donor and acceptor NBOs: LP indicates 1-center valence lone pair, and BD^* 2-center antibond. The arrows point to the charge transfer acceptor (which is the XB or HB donor).

2.2 Detailed results of the NBO analysis per type of $X\cdots Y$ interaction.

Table S1. Relation of two-electron stabilization energies (kcal/mol) for Br \cdots O, lateral Br \cdots Br and frontal Br \cdots Br interactions as obtained from NBO perturbation theory energy analysis of **Br₂-C₆H₃-OMe** dimers G, F and A, respectively. The labels CR, LP, BD(*) and RY(*) indicate, respectively, core, one-centre valence lone pair, two-centre (anti)bond, and Rydberg (anti)bond type of the donor and acceptor NBOs.

Dimer	Donor	NBO type(s)	Acceptor	NBO type(s)	E(2) (kcal/mol)
Br \cdots O (dimer G)	(C)Br (8)	BD , LP, CR	(C)O (25)	RY* , BD*	0.96
	Br (8)	LP , CR	CH	BD* , RY*	2.33
	O (25)	LP	(C)Br (8)	BD* , RY*	2.39
Br \cdots Br (dimer F)	(C)Br (8)	CR , BD	Br (24)	RY*	0.76
	Br (8)	LP , CR	C(20)H(29)	BD* , RY*	3.48
	Br (24)	LP , CR	(C)Br (8)	BD* , RY*	3.17
Br \cdots Br (dimer A)	Br (7)	LP , CR	(C)Br (23)	BD* , RY*	1.3
	Br (8)	CR	Br (24)	RY*	0.46
	Br (8)	LP , CR	C(22)-H(30)	BD* , RY*	4.82
	C(1)-H(12)	BD	C(22),H(30)	BD* , RY*	0.39
	Br (23)	CR	Br (7)	RY*	0.46
	Br (24)	LP , CR	Br (8)	BD* , RY*	1.29
	Br (23)	LP , CR	C(1), H(12)	BD* , RY*	4.82
	C(22)H(30)	BD	C(1) H(12)	BD* , RY*	0.39

Section 3. One-dimensional periodic DFT calculations

3.1 One-dimensional $Br_2-C_6H_3-OMe$ optimized structures

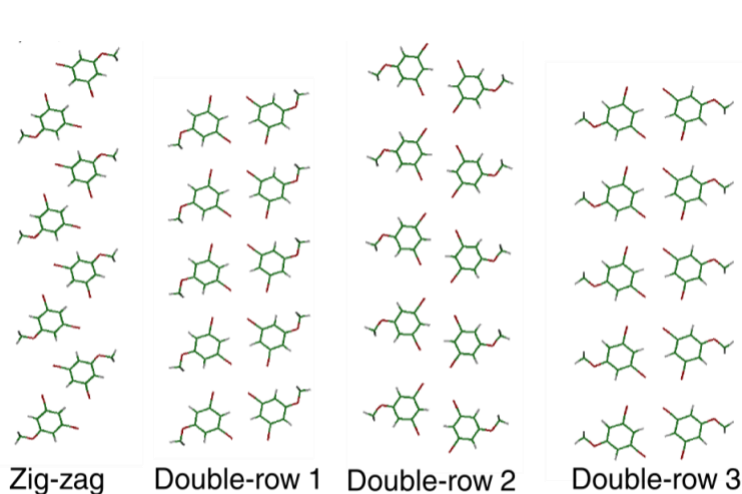


Figure S2. Optimized geometries of the four $Br_2-C_6H_3-OMe$ one-dimensional structures considered here.

3.2 Binding energy and geometrical parameters of one-dimensional $Br_2-C_6H_3-OMe$ optimized structures

Table S2. Energetic and structural data of the one-dimensional periodic DFT calculations on the Br_2PhOMe zig-zag, double-row 1, 2 and 3 structures shown in **Figure S2**.

	Zig-Zag	Double-row 1	Double-row 2	Double-row 3
Interaction E per molecule (kcal/mol)	-1.9	-3.64	-1.45	-2.01
Linear density (molecules/nm)	0.84	1.22	1.09	1.21
Side Br- -Br distance (Å)	5.26	3.54	3.53	3.47
Estimated φ	109	138	113	98
Lattice vector a (Å)	11.86	8.22	9.14	8.25

The lattice parameter and molecular geometry optimizations were carried out at the M062X/6-31g* (ultrafine, tight) level, using LanL2DZ on Br atoms (DFT1). Then, 5-dimer clusters obtained from replicating the 1D periodic dimers obtained in the previous step were generated and single-points energies were calculated on them using a DZ basis set (M062X/6-31g**), LanL2DZ on Br atoms and counterpoise basis-set superposition error correction. Deformation energies lay below 0.1 kcal/mol in all cases.

Section 4. Additional STM data

4.1 Large-scale STM images of $\text{Br}_2\text{-C}_6\text{H}_3\text{-OC}_n$ derivatives

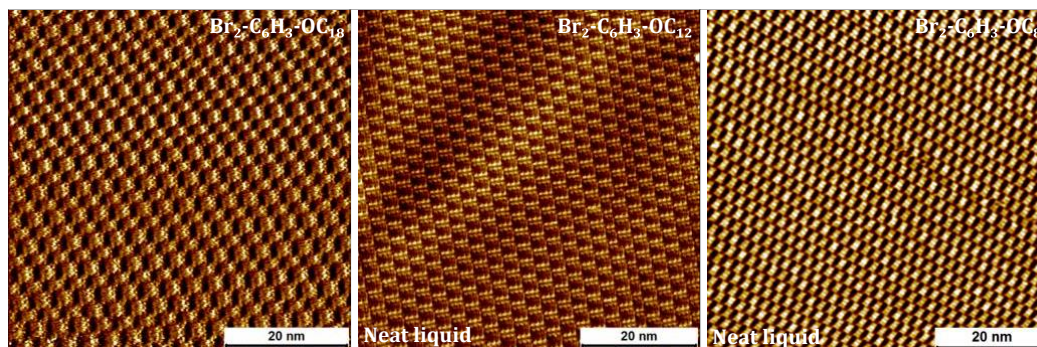


Figure S3. Large-scale STM images of the $\text{Br}_2\text{-C}_6\text{H}_3\text{-OC}_n$ derivatives at the liquid-solid interface. $\text{Br}_2\text{-C}_6\text{H}_3\text{-OC}_{18}$ was deposited as a 2×10^{-3} M solution in 1-phenyloctane whereas $\text{Br}_2\text{-C}_6\text{H}_3\text{-OC}_8$ and $\text{Br}_2\text{-C}_6\text{H}_3\text{-OC}_{12}$ were deposited as neat liquids. (As mentioned in the main text, the alternating hexamer-tetramer structure resembles a type of brickwork called the Flemish bond. “The Flemish bond is a type of brickwork in which ‘long’ and ‘short’ sections alternate in each row of bricks, with the positions of the ‘long’ and ‘short’ sections themselves alternating in neighbouring rows.”)

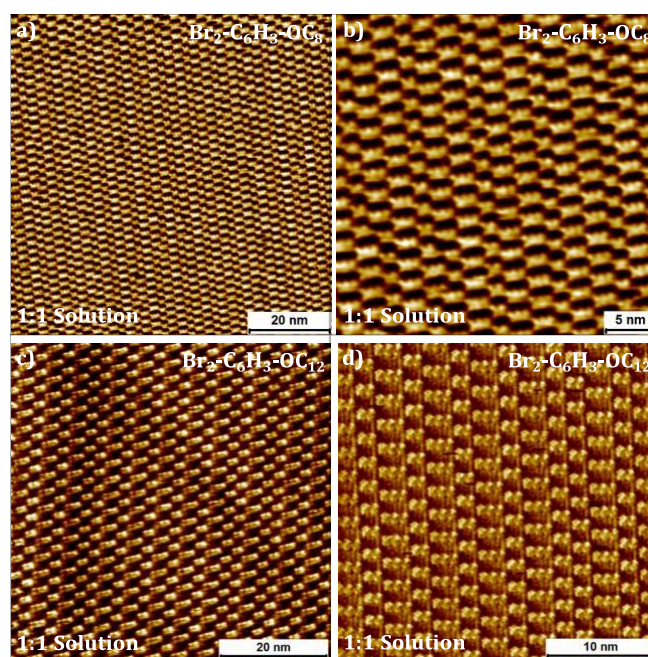


Figure S4. STM images of $\text{Br}_2\text{-C}_6\text{H}_3\text{-OC}_8$ (a, b) and $\text{Br}_2\text{-C}_6\text{H}_3\text{-OC}_{12}$ (c, d) obtained from 1:1 (v/v) solutions in 1-phenyloctane. The images clearly show that the percentage of tetramers increases upon dilution and the packing arrangement changes to alternating hexamers/tetramers.

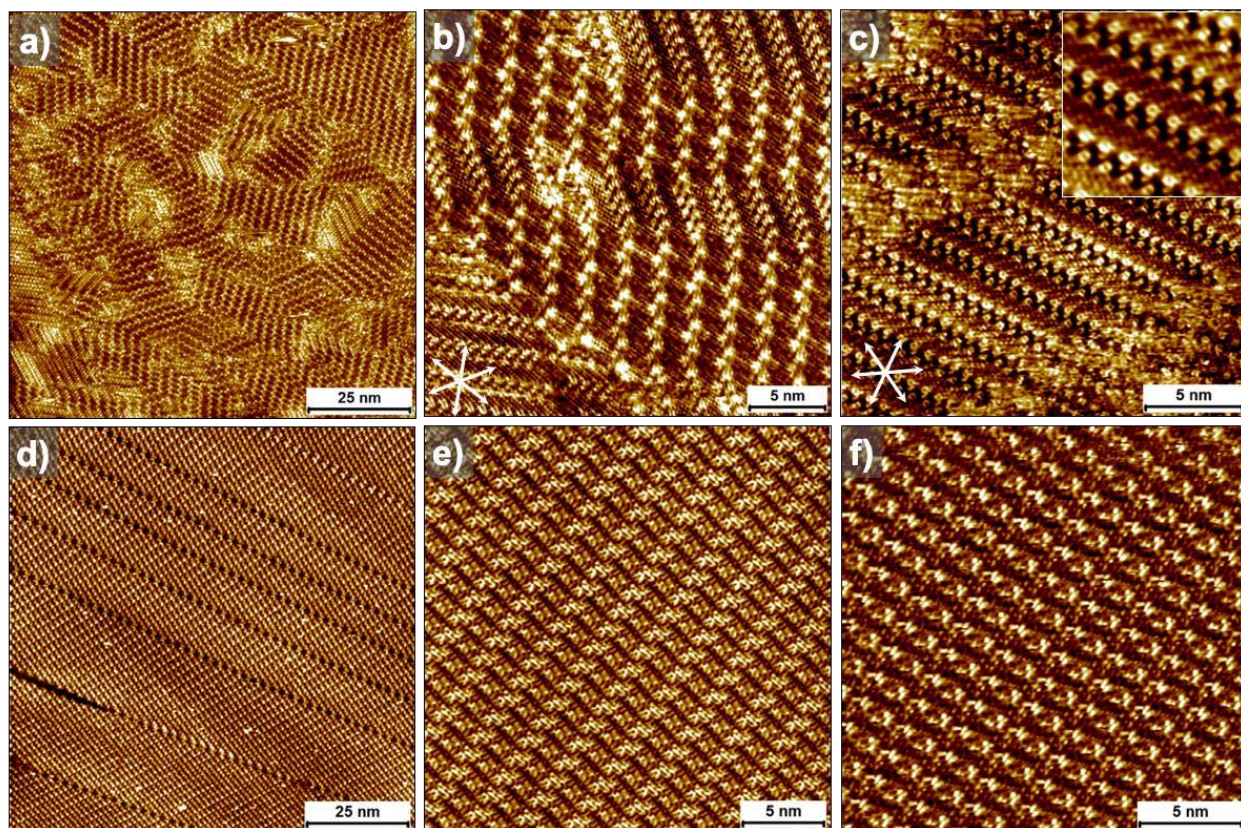


Figure S5. Additional STM data on $\text{Br}_2\text{-C}_6\text{H}_3\text{-OC}_{12}\text{O-C}_6\text{H}_3\text{-Br}_2$ and $\text{ISA-OC}_{12}\text{O-ISA}$ derivatives. (a) Large scale STM image of the monolayer formed by $\text{ISA-OC}_{12}\text{O-ISA}$ at the octanoic acid/HOPG interface. Panels (b) displays a small scale STM image showing the co-existence two different polymorphs, namely zig-zag and double row. (c) STM image of the double row structure. (d) Large scale STM image of the $\text{Br}_2\text{-C}_6\text{H}_3\text{-OC}_{12}\text{O-C}_6\text{H}_3\text{-Br}_2$ monolayer at the 1-phenyloctane/HOPG interface. (e, f) Small scale STM images of $\text{Br}_2\text{-C}_6\text{H}_3\text{-OC}_{12}\text{O-C}_6\text{H}_3\text{-Br}_2$ showing a large variation in the STM contrast of molecules.

Section 5. Effect of the inclusion of the extra-site:

- Effect on dimer A-G interaction energies:

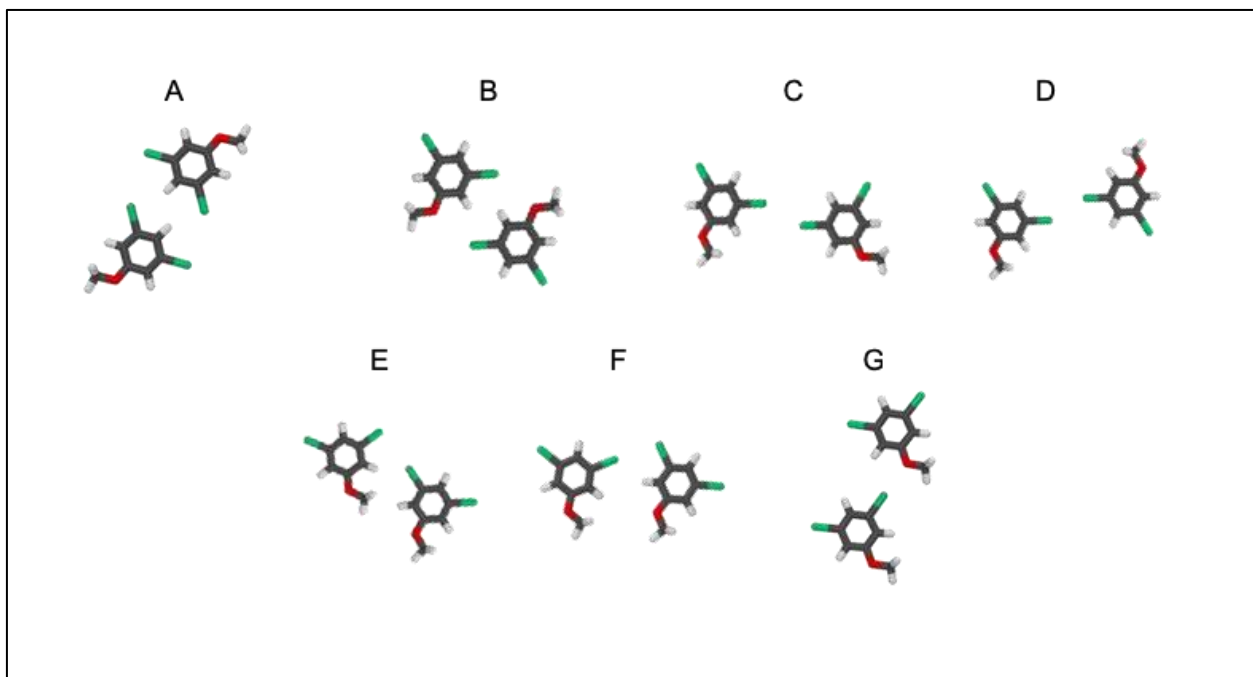


Table S3. Comparison of BSSE-corrected DFT interaction energies with molecular mechanics interaction energies for the set of **Br₂-C₆H₃-OMe** A-G dimers (see structures above), calculated with and without the extra-site (OPLSAA-x and OPLSAA, respectively).

	M06-2X/6-31g**	M06-2X/6-311++g**	OPLSAA	OPLSAA-x
A	-2.03	-1.82	-3.17	-2.85
B	-1.28	-1.18	-1.54	-1.89
C	-0.63	-0.68	-0.78	-0.83
D	-0.66	-0.68	-0.69	-0.74
E	-1.93	-2.01	-2.91	-3.03
F	-1.26	-1.40	-1.68	-1.89
G	-1.50	-1.84	-0.85	-1.59

The positive point charge to simulate the sigma hole in the MM calculations is necessary to reproduce not only the interaction energies but also the interatomic distances. With $x=0$, all Br \cdots Br and Br \cdots O distances are overestimated. For values of x of 0.035 or larger, interaction energies and interatomic distances are much closer to the obtained with DFT (with a margin of 0.5 kcal/mol and 0.1 Å or better). The interaction energies are least overestimated using $x=0.035$, and hence this value was selected to carry out the MM calculations.

Table S4. Comparison of intermolecular distances $d(X\cdots Y)$ (Å) on **Br₂-C₆H₃-OMe** A-G dimers optimized with DFT (M06-2X/6-31g**), OPLSAA, and OPLSAA-x. The columns labelled as $\Delta d(X\cdots Y)$ show the difference in equilibrium distances obtained with DFT and with each force-field method. The overall standard deviation of $\Delta d(X\cdots Y)$ for each method (σ) is shown at the bottom of the table.

Dimer	X \cdots Y	DFT $d(X\cdots Y)$	OPLSAA $d(X\cdots Y)$	$\Delta d(X\cdots Y)$	OPLSAA-x $d(X\cdots Y)$	$d(X\cdots Y)$
A	H \cdots H	2.70	4.40	1.7	2.7	0
B	H \cdots H	2.55	2.50	-0.05	2.5	-0.05
C	Br \cdots Br	3.58	4.00	0.42	3.7	0.12
D	Br \cdots Br	3.58	3.90	0.32	3.7	0.12
E	Br \cdots Br	3.82	3.90	0.08	3.9	0.08
F	Br \cdots Br	3.65	3.90	0.25	3.7	0.05
G	Br \cdots O	3.03	3.50	0.47	3.3	0.27
			σ	0.58	σ	0.10

-Effect on Br₂PhOC₈ hexamers:

Table S5. Total interaction energy and electrostatic contribution (kcal/mol) of a **Br₂-C₆H₃-OC₈** molecule embedded within two hexamers on a 80 X 80 graphene flake, calculated and without the extra-site (OPLSAA-x and OPLSAA, respectively).

	OPLSAA-x	OPLSAA
Interaction energy (kcal/mol)	-45.6813	-39.4337
Charge-charge	-0.9543	5.2892

Section 6. Alkyl chain orientation on graphene.

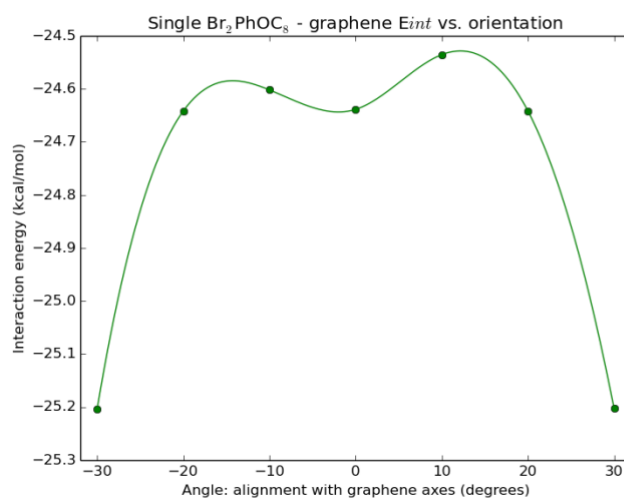


Figure S6. Interaction energy change (OPLSAA-x, kcal/mol) as a function of the alkyl chain-graphene axis angle for a $\text{Br}_2\text{-C}_6\text{H}_3\text{-OC}_8$ molecule. Angles 30 and -30 correspond to zig-zag alignment. The maximum difference is 0.7 kcal/mol per molecule.

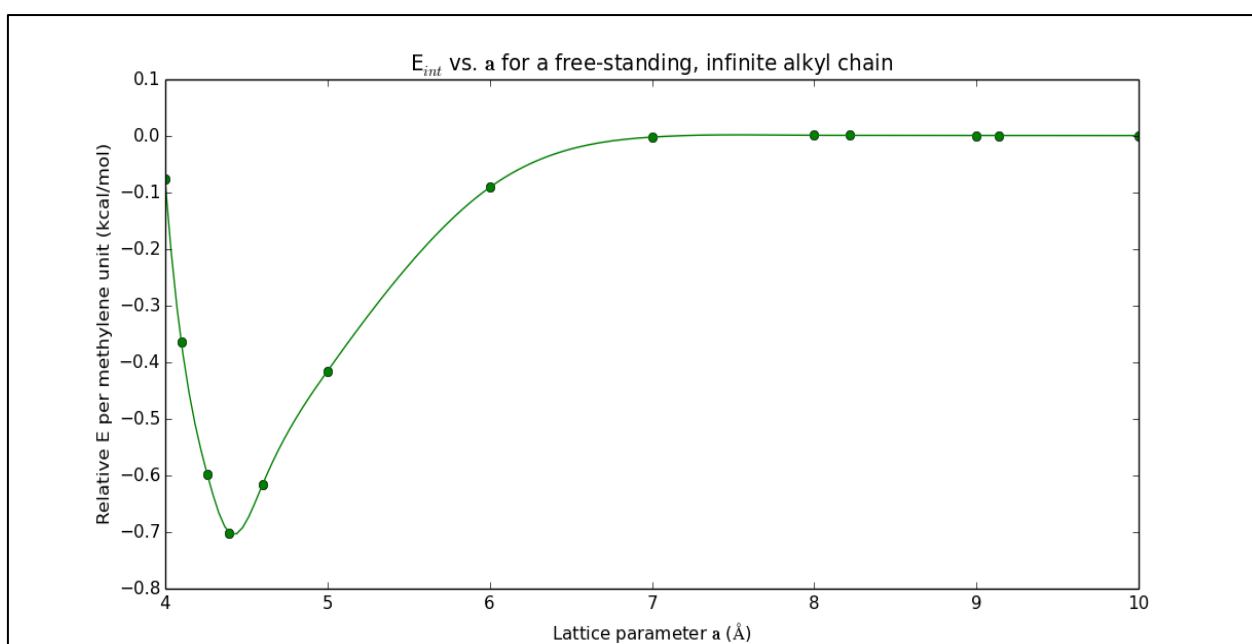


Figure S7. Interaction energy (E_{int} , kcal/mol) as a function of the distance between two infinite alkyl chains at the M062X/6-31G** level. The equilibrium distance (4.4 Å) and its corresponding interaction energy (0.9 kcal/mol per methylene) are in good agreement with the literature. [Tomanek, J. Chem. Phys.128, 124709, 2008].

Section 7. Periodic structure optimization and commensurability.

Creation of quasi-commensurate supercells

Most molecular-mechanics structures reported in this manuscript were obtained using periodic boundary conditions. In order to obtain equilibrium structures, not only the atomic positions were optimized but also the supercell lattice parameters (a , b and γ) together with the orientation with respect to the graphene surface (Γ). Thus, the problem of incommensurability between the graphene surface and the lattice parameters arises naturally. We designed an optimization algorithm aimed at avoiding (within a threshold) artefacts due to excessive compression or dilation of the molecular lattice or the graphene layer.

The algorithm proceeds as follows. First, a model for the adsorbed monolayer is constructed. This process starts from an optimized structure for an isolated form of the relevant initial cluster (e.g. a hexamer of $\text{Br}_2\text{-C}_6\text{H}_3\text{-OC}_3$). Then, for each specific combination of a , b , γ and Γ , a periodic initial structure is created, consisting of n repeated instances of this initial cluster. Next, a quasi-commensurate graphene supercell is built (*vide-infra*). Finally, this structure is optimized while keeping the graphene layer fixed, and its energy per surface area recorded. This operation was performed for a range of values of a , b , γ and Γ so as to ensure that the final structure was a minimum in all degrees of freedom.

The quasi-commensurate graphene supercells were generated using a numerical approach. A large enough multiple of the molecular layer lattice parameters was selected so that it would be similar to the graphene supercell within a margin of 1 Å (roughly 1 % of the smallest supercells). If the molecular lattice is oblique ($\gamma \neq 90$), superposition with a rectangular lattice such as that of graphene may create overlapped regions. This also was accounted for. The fortran code used to calculate this is shown at the end of this document.

Section 8. Estimation of alkyl chain contribution to stabilization

In MM, the contribution of parts of a structure to the overall stabilization (E_{int}) can be calculated. The atoms on a $\text{Br}_2\text{-C}_6\text{H}_3\text{-OC}_8$ or a $\text{Br}_2\text{-C}_6\text{H}_3\text{-OC}_{12}$ molecule were grouped into 'heads' (the $\text{Br}_2\text{-C}_6\text{H}_3\text{-O}$ moiety) and 'tails' (the alkyl chain), and the contribution of each group to the total E_{int} was calculated for the equilibrium line/hexamer/tetramer/dimer structures shown in Fig. 4 of the main text.

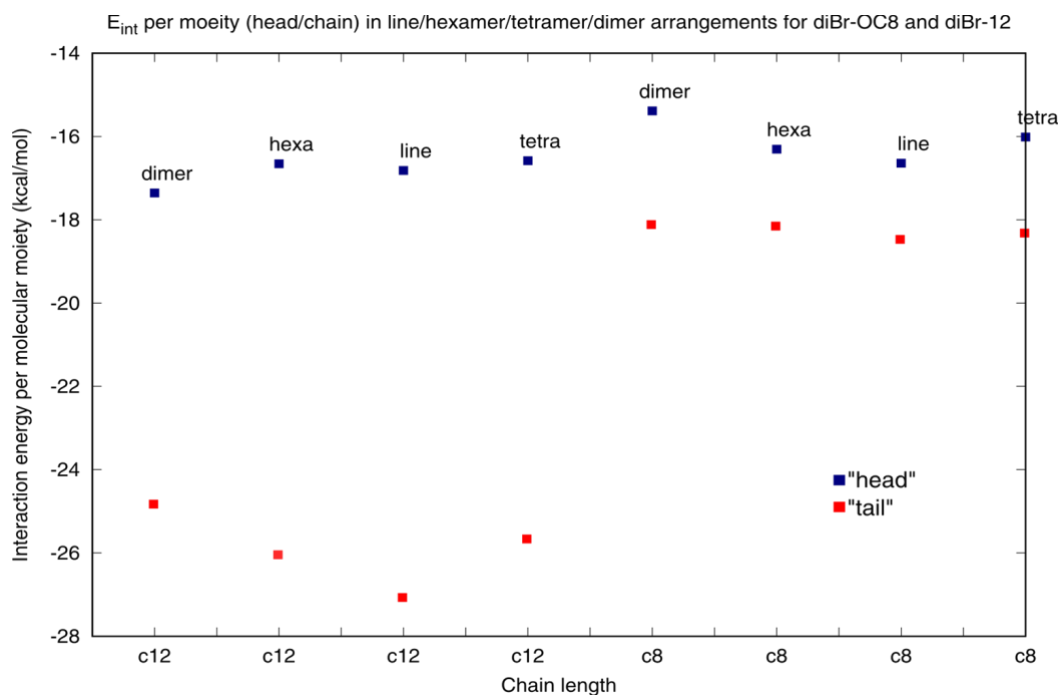


Figure S8. 'Heads' and 'tails' contributions to the E_{int} (kcal/mol per molecule) for $\text{Br}_2\text{-C}_6\text{H}_3\text{-OC}_8$ or a $\text{Br}_2\text{-Ph-OC}_{12}$, calculated with the x-site force-field. In $\text{Br}_2\text{-C}_6\text{H}_3\text{-OC}_8$, 'tails' contribute slightly above 50 %, while in $\text{Br}_2\text{-C}_6\text{H}_3\text{-OC}_{12}$, the percentage rises to about 60%.

Section 9. Alkylated isophthalic acid models

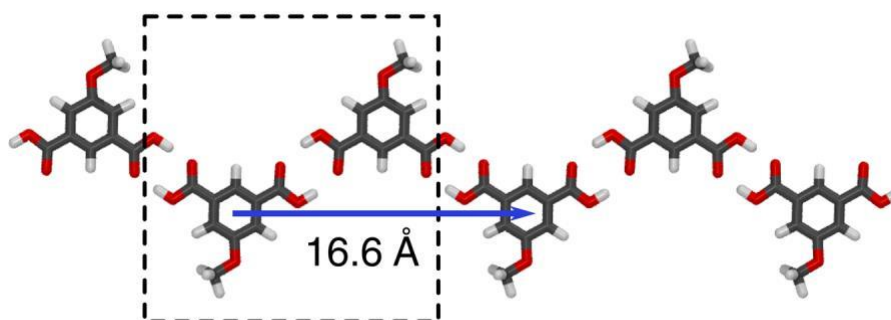


Figure S9. Periodic 1D zig-zag structure of ISA-OMe (DFT M062X/6-31g**). The 1D lattice parameter is in very good agreement with the molecular mechanics intra-row lattice parameter and the experimental lattice parameter b .

Section 10. Double row (DR) versus zig-zag (ZZ) structures of $\text{Br}_2\text{-C}_6\text{H}_3\text{-OC}_{12}\text{O-C}_6\text{H}_3\text{-Br}_2$

Table S6 below shows that the DR phase is more stable in vacuum in potential energy terms than the ZZ phase. However, at the solution-solid interface the ZZ phase can be stabilized via co-adsorbed solvent (1-phenyloctane) molecules. Note that the 1-phenyloctane molecules barely fit inside the open areas within the DR structure. However, in the ZZ phase, likely one (but it may be up to two) 1-phenyloctane molecule can stabilize the pore. The interaction energy per unit area of both phases seems of the same order of magnitude, and it may well be that lower entropy loss in the ZZ phase results in a more favourable free energy of self-assembly for the ZZ phase.

	E/molecule (kcal/mol)	Number of 1-PO molecules	d(R-R) (Å)	Area (nm ²)
Double row (DR)	-54	0	5.7	2.12
Zig-zag (ZZ)	-49*	1 or 2	10.5	3.17

*Interaction energy decreases by 9 or 20 kcal/mol (w.r.t no solvent at all) when 1 or 2 molecules of solvent reside in the pore, respectively (see **Figure S10** below). The interaction energy per surface area (MM/OPLSAA-x) is 25.5 kcal/mol per nm² for the DR structure, and 15.5, 18.3 and 21.7 kcal/mol per nm² for the ZZ including no solvent, one 1-phenyloctane molecule, and two 1-phenyloctane molecules.

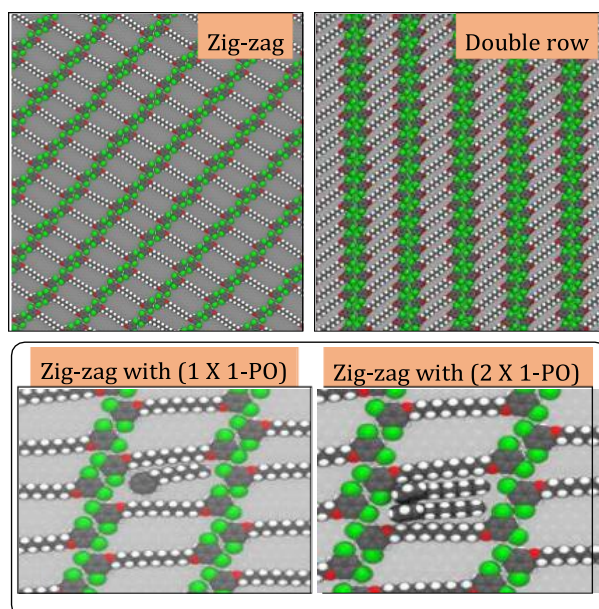


Figure S10. Experimentally observed zig-zag and hypothetical double-row structure for $\text{Br}_2\text{-C}_6\text{H}_3\text{-OC}_{12}\text{O-C}_6\text{H}_3\text{-Br}_2$. Lower panels show the zig-zag structure with co-adsorbed 1-phenyloctane molecules.

Computational details: One and two 1-phenyloctane molecules were added in the open areas of the ZZ phase, and their structures were optimized keeping the molecular network and graphite frozen. Single point energies were then calculated for the zero, one and two 1-phenyloctane containing structures, including only the **Br₂-C₆H₃-OC₁₂O-C₆H₃-Br₂** molecular network and its intermolecular interactions with surface and 1-phenyloctane molecules. All calculations were carried out using periodic MM (OPLSAA-x).

Appendix. Program to calculate commensurability between two lattices

```

!
!ANA SANZ MATIAS, Leuven 2015
!
! | I
! | I
! Gamma I
! |---I \gamma I
! | I \ I | wedge (90 - gamma - Gamma)
! | I I |
! I |
!
! Program to find out the (approximate) commensurability of two 2D
lattices.
! Lattice A is graphene/graphite. The "unit cell" used here is actually
a 4 atom supercell with gamma=90.
! Lattice B is characterized by two lattice vectors (a and b, also called
"a" and "b" in the code) and an angle, gamma ("gam").
! There is an extra parameter: Gamma, the angle between both lattices
(see ascii scheme, called "angle").

! It works with an input file that contains: a; b; gamma; Gamma; threshold
1 and threshold 2.
! Thresholds are in AA. Threshold 1 (thres) is the difference between
the graphene supercell length and the projected monolayer supercell
length in directions a and b. Threshold 2 (thres2) is the difference in
the
! Ideally, to achieve complete commensurability, both thresholds should
be zero. Increase at your own risk.
! As output, it provides the number of copies of B unit cell, as well as
graphene unit cell, to achieve commensurability according to the
thresholds set in the input. A few extra quantities are provided to
assess the harshness of the approximation. Depending on lattice B, unit
cell overlap can happen when building the supercell. The number and
direction of overlapping B unit cells is also provided in the output.

!Compilation: $compiler commens.f90 -o commens.x ; I used gfortran as
compiler.
!Run: ./commens.x < input.txt > output.dat
!Input:

!a
!b
!gamma
!Gamma
!angle
!threshold 1
!threshold 2

```

```

program trans
implicit none
integer :: j, k, gcells, mcells
real :: a, b, angle, convfac, catoms, gam, aglength, amlength, bglength,
bmlength, thresh, wedge, thresh2, wedgeb
integer, parameter :: iunit=55, ounit=66
real, allocatable :: C(:,:), F(:,:), G(:,:)
real, dimension(3) :: va, vb
character(len=3), allocatable :: label(:)
real, parameter :: agraph=2.45951, bgraph=4.26

!Open input and read it:
read(*,*) a
read(*,*) b
read(*,*) gam
read(*,*) angle
read(*,*) thresh
read(*,*) thresh2
!conversion factor degrees to radians
convfac=3.1415926535/180

!Total length on x and y:

do gcells=1,1111
  do mcells=2,1111
    aglength=agraph*gcells
    wedge=a*mcells*sin((90-gam-angle)*convfac)
    amlength=a*sin((gam+angle)*convfac)*mcells-wedge/tan((90 -
angle)*convfac)
    if(abs((aglength-amlength)).le.thresh) then
      do j=0,1111
        if((abs(wedge-j*b*cos(angle*convfac))).le.thresh2) then
          write(*,*) 'agrphlength', aglength, 'amonolength', a
mlength, 'graphene cells a ', gcells, 'monolayer cells a
', mcells
          goto 100
        else
          cycle
        endif
      enddo
    endif
  enddo
enddo
100 do gcells=1,11130
  do mcells=3,11190
    bglength=bgraph*gcells
    wedgeb=b*mcells*sin((angle)*convfac)
    bmlength=b*cos(angle*convfac)*mcells
    wedgeb/tan((gam+angle)*convfac)
    if(abs((bglength-bmlength)).le.thresh) then
      do k=0,18

```

```

        if((abs(wedgeb-
k*a*sin((gam+angle)*convfac))).le.thresh2) then
            write(*,*)'bgraphlength',bglength,'bmo
nolength',bmlength,'graphene      cells      b
',gcells,'monolayer cells b' ,mcells
            write(*,*)'adiff      ', abs((aglength-
amlength)), 'bdiff      ', abs((bglength-
bmlength))
            write(*,*)
            write(*,*) ' wedge a ', wedge ,
'projected b', j*b*cos(angle*convfac)
            write(*,*) ' wedge b ', wedgeb ,
'projected a', k*a*sin((gam+angle)*convfac)
            write(*,*)'wedge a diff', (abs(wedge-
j*b*cos(angle*convfac))), 'wedge      b
diff', (abs(wedgeb-
k*a*sin((gam+angle)*convfac)))
            write(*,*)
            write(*,*) 'overlapped      a      ',
wedge/(b*cos(angle*convfac)),
nint(wedge/(b*cos(angle*convfac)))
            write(*,*) 'overlapped      b',
wedgeb/(a*sin((gam+angle)*convfac)),
nint(wedgeb/(a*sin((gam+angle)*convfac)))
            write(*,*) 'Area excess (A_m/A_G) '
            write(*,*)
            amlength*bmlength/(aglength*bglength)
            stop
        else
            cycle
        endif
    enddo
enddo
enddo
end program

```